

Dynamics Underlying Synaptic Gain Between Pairs of Cortical Pyramidal Neurons

Kara G. Pratt,^{*†} Christine E. Taft,^{*} Michelle Burbea,^{††} Gina G. Turrigiano

Department of Biology and Center for Behavioral Genomics, Brandeis University, Waltham, Massachusetts 02454

Received 7 May 2007; accepted 29 August 2007

ABSTRACT: Changes in connectivity between pairs of neurons can serve as a substrate for information storage and for experience-dependent changes in neuronal circuitry. Early in development, synaptic contacts form and break, but how these dynamics influence the connectivity between pairs of neurons is not known. Here we used time-lapse imaging to examine the synaptic interactions between pairs of cultured cortical pyramidal neurons, and found that the axon–dendrite contacts between each neuronal pair were composed of both a relatively stable and a more labile population. Under basal conditions, loss and gain of contacts within this labile population was well balanced and there was little net change in connectivity.

Selectively increasing the levels of activated CaMKII in the postsynaptic neuron increased connectivity between pairs of neurons by increasing the rate of gain of new contacts without affecting the probability of contact loss, or the proportion of stable and labile contacts, and this increase required Calcium/calmodulin binding to CaMKII. Our data suggest that activating CaMKII can increase synaptic connectivity through a CaM-dependent increase in contact formation, followed by stabilization of a constant fraction of new contacts. © 2007 Wiley Periodicals, Inc. *Develop Neurobiol* 68: 143–151, 2008

Keywords: synaptic plasticity; CaMKII; synaptic turnover

INTRODUCTION

The activity-dependent refinement of cortical circuitry is thought to occur, in part, through structural changes in the connectivity between neurons. Early in the development of central neural circuits, synap-

ses are highly dynamic, with new synapse formation and synapse loss occurring simultaneously (Bonhoeffer and Yuste, 2002). The physical interactions between axons and dendrites that underlie these processes are only poorly understood, due to the difficulty of simultaneously imaging both structures in living tissue. In contrast, the dynamics of postsynaptic spine and filopodial motility have been well described and quantified, and can occur over both rapid and slow time scales (Wong and Wong, 2000; Bonhoeffer and Yuste, 2002; Yuste and Bonhoeffer, 2004). Rapid (seconds to minutes) changes in spine shape can occur without apparent loss of contact with presynaptic structures (Konur and Yuste, 2004; Deng and Dunaevsky, 2005; Umeda et al., 2005), and while the function of this spine “morphing” is not fully understood, changes in spine shape and size are correlated with changes in synaptic strength (Matsuzaki et al., 2004; Zhou et al., 2004). Spine and filopodial formation and retraction events occur over longer time

This article contains supplementary material available via the Internet at <http://www.mrw.interscience.wiley.com/suppmat/1932-8451/suppmat/>

*These authors contributed equally to this work.

[†]Present address: Department of Neuroscience, Brown University, Providence, Rhode Island.

^{††}Present address: Fuld and Company, 126 Charles St., Cambridge, Massachusetts.

Correspondence to: G.G. Turrigiano (turrigiano@brandeis.edu).

Contract grant sponsor: National Science Foundation; contract grant number: IBN 023519.

Contract grant sponsor: National Institute of Health; contract grant number: NS 36853.

© 2007 Wiley Periodicals, Inc.

Published online 18 October 2007 in Wiley InterScience (www.interscience.wiley.com).

DOI 10.1002/dneu.20577

scales (minutes to days) and are thought to reflect synapse formation and loss, respectively (Grutzendler et al., 2002; Trachtenberg et al., 2002; Yuste and Bonhoeffer, 2004). In cortical circuits, spine/filopodial turnover can be modulated by manipulations of sensory experience (Trachtenberg et al., 2002; Majewska and Sur, 2003; Zuo et al., 2005), and this motility is downregulated in the adult cortex (Grutzendler et al., 2002; Trachtenberg et al., 2002), suggesting that spine/filopodial turnover may contribute to circuit remodeling during early development.

Despite this growing literature on spine/filopodial turnover, we do not know how (or whether) these dynamics translate into changes in connectivity between pre- and post-synaptic partners. If unitary connections between most synaptic partners have a labile population of contacts, then changing the rates of formation or loss within this labile population could serve as a substrate for structural synaptic plasticity. Developmental or activity-driven changes in unitary synaptic connectivity could be achieved through increased stabilization of existing contacts, or through enhanced formation of new contacts, or both—but which (if any) of these mechanisms are utilized within developing cortical circuits is unknown. To begin to address these questions, we used time-lapse imaging to examine synaptic contact formation and loss between pairs of young cultured cortical pyramidal neurons, during a manipulation (elevation of activated postsynaptic CaMKII) that is known to increase neuronal connectivity (Pratt et al., 2003).

METHODS

Transfection of Cortical Cultures

Visual cortical cultures were prepared as described previously from P3–5 Long-Evans rat pups (Watt et al., 2000; Pratt et al., 2003). At 6–7 days *in vitro* (DIV) cultures were transfected using the LipofectAmine 2000 reagent (Invitrogen, Carlsbad, CA). Cultures were transfected separately with DsRed (using the N1-DsRedT4 vector, gift of Dr. B. Glick) to illuminate presynaptic axons, and with either PSD-95-EGFP alone (to illuminate postsynaptic sites, Control), or PSD-95-EGFP + T286D as described previously (Pratt et al., 2003). In some experiments, GluR2-EGFP was used in place of PSD-95 as a postsynaptic marker. Lipofectamine transfection was optimized for low efficiency to maximize the chances of finding a single transfected axon interacting with a single transfected postsynaptic partner. PSD-95-EGFP expression provides a sufficient background level of illumination to allow visualization of the entire transfected neuron including thin dendritic filopodia [Fig. 1(A)].

Time-Lapse Imaging

About 14–16 h after transfection, cultures were moved to an Olympus IX70 microscope and perfused with oxygenated ACSF (126 mM NaCl, 5 mM KCl, 1 mM NaHPO₄, 25 mM NaHCO₃, 2 mM CaCl₂, 14 mM glucose) at 33°C. The dish was scanned until a pair of transfected neurons was found. To be chosen for imaging, a pair of neurons had to meet the following criteria: both the pre- and postsynaptic neurons had to display classic pyramidal morphology (Watt et al., 2000), the presynaptic neuron had to be expressing DsRed, the postsynaptic neuron had to be expressing PSD-95-EGFP, and the presynaptic axon had to contact the postsynaptic neuron one or more times. Thus, we imaged pairs of neurons that had already established connections at the time of imaging. Generally, it was possible to capture all the axon–dendrite interactions within a single field of view.

Axon–dendrite interactions were visualized with an oil-immersion 60× lens (n.a. 1.25), and images were taken using a cooled CCD camera (Orca ER, Hamamatsu) controlled with Improvise software. The pixel size was 0.11 × 0.11 μm². Z-stacks of images 0.2 μm apart were taken using a z-section focus drive, first with a GFP filter and then with a DsRed filter; 6–12% neutral density filters were used to reduce bleaching. The selected field of view was imaged approximately every 20 min for 1.5–3 h. Maximal projections of Z stacks at the two wavelengths were overlaid and analyzed at each time point. Sites where axons and dendrites were in contact (or within 1 pixel of each other) and the PSD-95 fluorescence was >25% above the local background were considered to be putative synaptic contacts. The area of each such PSD-95 punctum was quantified from all contiguous pixels that were >25% above background. The number of gain and loss events were quantified at each time point and converted into rates by dividing by elapsed time; these values were then averaged across time points for each pair. The absolute rates of loss and gain will depend on the sampling interval; to verify that our measure of the ratio of loss to gain was not affected by under-sampling, in four pairs we sampled every 10 min and compared the ratios obtained by including every time point (10-min interval) and every other time point (20-min interval); the ratios obtained were not significantly different (1.3 ± 0.1 vs. 1.6 ± 0.4, *p* = 0.54). The net change in contact number was determined by subtracting the number of contacts at the beginning of the experiment (at *t* = 0) from the number at the end of the experiment and dividing by the total number of hours imaged to give the net change/hour. For experiments in which colocalization of markers were quantified (Fig. 2) only puncta where fluorescence was >25% above the local background were included. Immunohistochemistry against synaptic markers, and FM1-43 labeling, was performed and analyzed as described previously (Wierenga et al., 2005, 2006).

Statistics

Statistical significance between conditions was determined using unpaired two-tailed Student's *t* tests except where

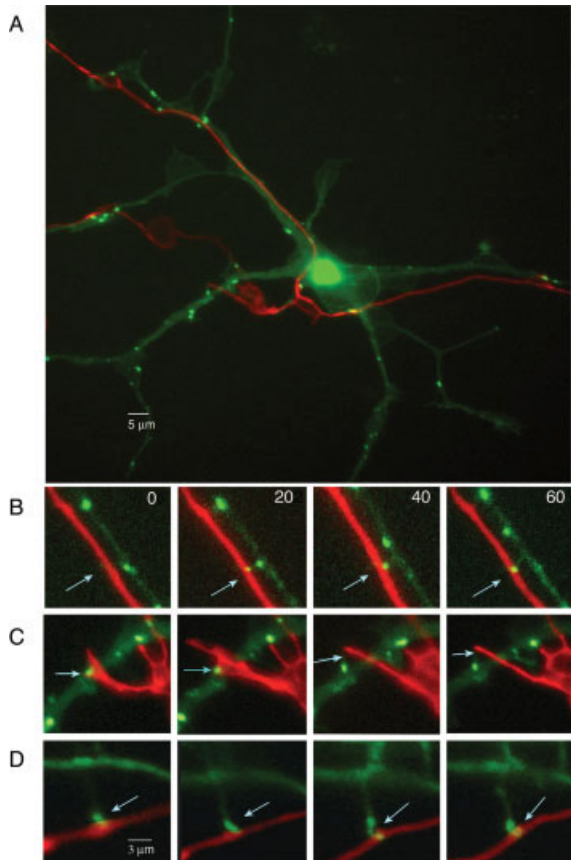


Figure 1 Imaging contact formation and loss between pairs of cortical pyramidal neurons. (A) Postsynaptic neuron expressing PSD-95-EGFP (green), and presynaptic axon expressing DsRed (red). Sites of axon-dendrite contact that accumulate PSD-95 (green puncta) can be readily identified. (B) Contact formation. The arrow shows a site where initially there is no contact ($t = 0$); at $t = 20$ min a dendritic protrusion has contacted the axon and PSD-95 has begun to accumulate; this accumulation increases and persists. (C) Contact loss. Arrow marks the site where an initial contact ($t = 0$ and 20) is lost at subsequent times ($t = 40$ and 60). (D) A persistent contact. The arrow marks the site where a dendritic protrusion is in contact with an axon and has accumulated PSD-95; this contact persisted throughout the time series. Time signature in minutes.

noted. When we compared the rates of gain and loss for each pair within a condition, paired t tests were used. Because the distributions deviated significantly from normal, the non-parametric Mann-Whitney test was used to determine differences in % stable contacts and contact lifetimes.

RESULTS AND DISCUSSION

Cultures (made from P3 rat pups, transfected after 6–7 DIV) were transfected separately at low efficiency

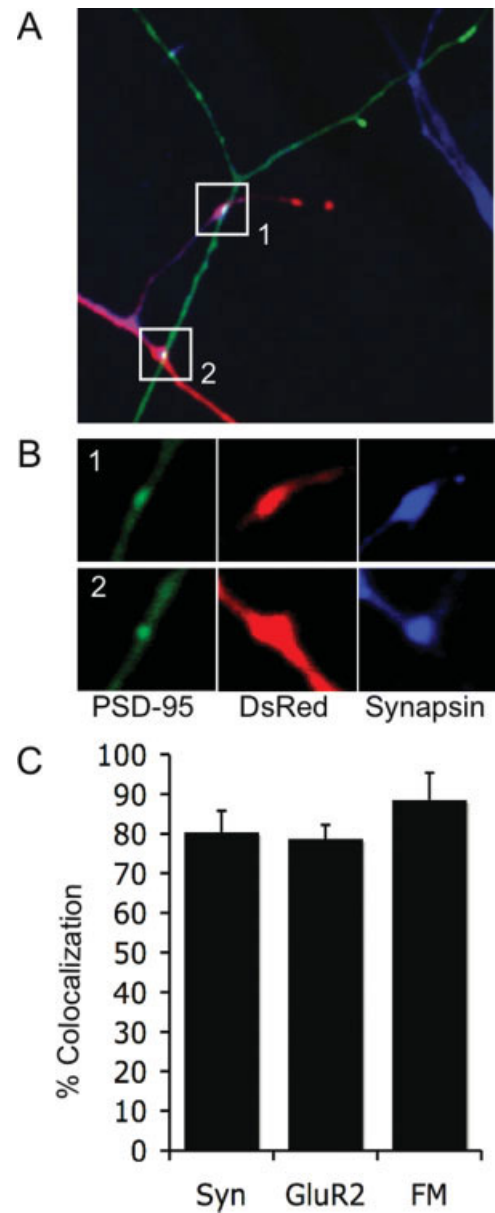


Figure 2 Sites of contact that accumulate PSD-95 are well colocalized with other synaptic markers. (A) Example of an axon-dendrite interaction, counter-stained against the presynaptic marker Synapsin. Axon contains soluble DsRed (red), the dendrite expresses PSD-95-EGFP (green), and the Synapsin label is shown in blue. Boxes 1 and 2 highlight sites of contact. (B) Separate channels for all three markers are shown for the regions highlighted in boxes 1 and 2 above, illustrating the accumulation of PSD-95 and Synapsin at sites of contact. (C) The % colocalization between sites of contact that accumulate PSD-95 and three synaptic markers: FM1-43, the AMPA receptor subunit GluR2, and Synapsin.

Table 1 Categories of Contact Formation and Loss

	Contact Gain (%)		Contact Loss (%)	
	Control	T286D	Control	T286D
Dendrite	27	41	41	44
Axon	7	4	14	16
Both	21	22	11	16
Formation/loss of PSD-95 puncta	45	33	34	24

The percent of contact gain and loss events in which the primary movement was the dendrite, the axon, or both. An alternative form of contact gain or loss occurred when axonal and dendritic structures remained in apparent contact (as assessed from the background dendritic fluorescence), but a PSD-95 puncta formed *de novo* (for a contact gain event) or disappeared (for a contact loss event). Differences between frequencies for control and T286D were not significant (Pearson's χ^2 test). A fraction of events were ambiguous and were not classified.

with DsRed to visualize presynaptic neurons and their axons, and with PSD-95-EGFP to visualize dendrites containing postsynaptic PSD-95 puncta. In these cultures, each pyramidal neuron receives inputs from many presynaptic partners. Low efficiency transfection (only a few neurons/dish) allowed us to find postsynaptic neurons that were contacted by only one DsRed-labeled axon, so we could follow contact formation and loss between individual pairs of pyramidal neurons [imaged every 20 min, generally for 2–3 h; Fig. 1(A)]. As is normal for these young cortical neurons, many of these contacts were formed onto filopodial or spine-like dendritic structures [Fig. 1(B,D); 49% of contacts, $n = 5$ pairs], whereas others were formed onto dendritic shafts [Fig. 1(C); 51% of contacts, $n = 5$ pairs]. PSD-95 is one of the first synaptic proteins to accumulate at nascent excitatory synapses (Cohen-Cory, 2002; Niell et al., 2004; Waites et al., 2005), and has previously been used as a marker for putative excitatory postsynaptic sites in live imaging studies (Marrs et al., 2001; Ebihara et al., 2003). To quantify the percent of PSD-95 positive axon–dendrite contacts that also cluster other pre- and postsynaptic markers, we stained cultures against the presynaptic marker synapsin ($80.4\% \pm 5.3\%$ colocalization, 12 pairs), or the GluR2 subunit of the AMPA receptor ($78.7\% + 3.4\%$ colocalization, 18 pairs; Fig. 2). We also quantified the percent of contacts capable of presynaptic vesicle recycling by labeling with FM1-43 ($88.5\% \pm 6.8\%$, 5 pairs; Fig. 2). These rates of colocalization agree well with previous data from our lab (Pratt et al., 2003), and suggest that the great majority of these contacts represent functional synaptic sites.

Any incidence in which the axon and dendrite formed a new such site of contact was considered to be a “gain” event [Fig. 1(B)]. Conversely, any time such a site was lost was considered to be a “loss” event [Fig. 1(C)]. Finally, initial contacts that persisted throughout the duration of the experiment were considered “stable” [Fig. 1(D)]. Loss events fell into two distinct categories: those in which the axons and

dendrites stayed in contact but the PSD-95 punctum disappeared (35% of cases), and those in which the PSD-95 punctum persisted but the axon and dendrite separated. In the majority of the later cases, the dendrite appeared to move away from the more stable axon, or both axon and dendrite moved apart, whereas only rarely did dendritic structures appear stationary while axons moved (Table 1). Like contact loss, contact formation usually involved the dendrite or dendritic protrusions moving toward a more stable axon [Fig. 1(B), Table 1] or the axon and dendrite moving toward each other, followed by formation or movement of a PSD-95 puncta to the site of contact. Although we have not followed these movements with high temporal resolution, these observations are in agreement with previous imaging studies in suggesting a high degree of dendritic motility (Jontes et al., 2000) that often exceeds that of the axon (Deng and Dunaevsky, 2005).

To quantify the dynamics of contact gain and loss, we began by examining the synaptic interactions between pairs of pyramidal neurons under “basal” conditions ($n = 14$ pairs, with 86 initial contacts). We found that each pair examined had both a relatively stable (present throughout the experiment) and a more labile population of contacts. For each pair the majority (about 75%) of contacts present at the beginning of the experiment were stable over the imaging period, while the remainder of the initial contacts were labile and were lost at some point during the imaging period [Fig. 3(A)]. Of these labile contacts, the average lifespan was 34 ± 5 min. To determine whether the magnitude of the PSD-95 signal at sites of contact was correlated with retention or loss of contacts, we quantified the area of the punctate PSD-95 signal at all contacts at the beginning of the experiment, and then divided them into stable and labile populations depending on whether they were subsequently lost or maintained. There was no difference in average pixel area between stable and labile contacts [Fig. 3(B)].

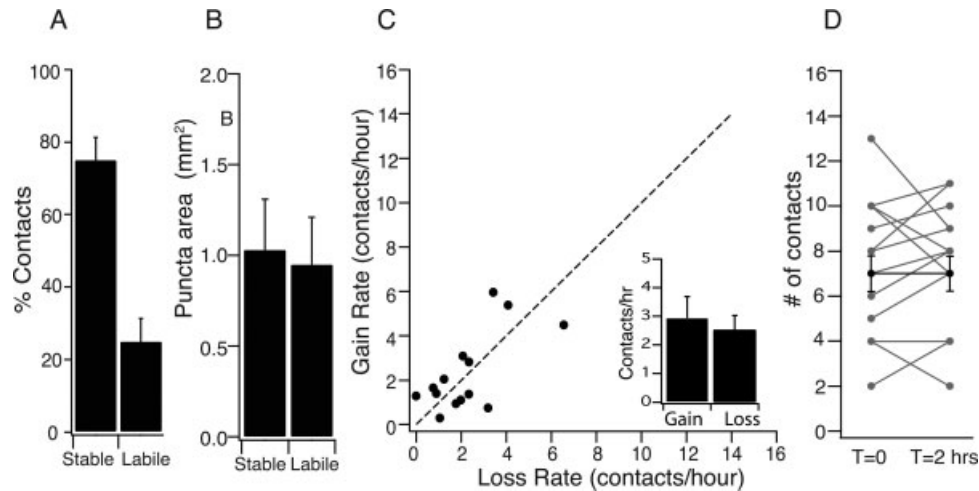


Figure 3 Turnover of synaptic contacts. (A) The proportion of stable (present throughout the imaging period) and labile (lost at some point during the imaging period) contacts calculated for each pair and then averaged across pairs ($n = 14$ pairs). (B) The average area of the PSD-95 puncta for stable and labile contacts. (C) The rates of contact gain and loss, plotted for each pair. The dashed line indicates unity (equal rates of gain and loss). Inset: rates of gain and loss averaged across pairs. (D) Number of contacts for each pair over the course of the imaging period. Gray circles: individual pairs at $t = 0$ and $t = 2$ h. Black circles: average number of contacts at $t = 0$ and $t = 2$ h.

Control pairs with low rates of contact loss also, on average, had low rates of contact gain [Fig. 3(C,D)]. When the average rates of gain and loss were plotted against each other for each pair, control pairs were close to evenly distributed above and below the unity line (representing equal rates of gain and loss), and on average these two rates were not different from each other [Fig. 3(C), inset]. As a consequence, there was little net change in connectivity over the imaging period [Fig. 3(D)]. These data indicate that the synaptic connections between single pairs of pyramidal neurons consist of both a relatively stable and a more transient group of contacts. The transient connections undergo a basal level of formation and elimination, and the rates of these two processes are well balanced so that the net change in connectivity is small. In a second set of experiments, we used tagged GluR2 ($n = 9$) rather than PSD-95 to image contact turnover; we obtained similar results, and the rates of contact formation and loss were not significantly different with these two synaptic markers (loss: GluR2, 2.5 ± 0.6 and PSD-95, 2.5 ± 0.5 ; gain: GluR2, 2.0 ± 0.5 and PSD-95, 2.9 ± 0.8).

It has been suggested that changes in connectivity may be relatively insensitive to global changes in activity, but rather may be driven by relative differences in synaptic activation (Hua et al., 2004). The reported effects on cortical spine motility of manipulating overall levels of activity (or of glutamate receptor

activation) *in vitro* have been mixed, with some studies observing changes while others have not (Dunaevsky et al., 1999; Fischer et al., 2000; Oray et al., 2006). However, the effects of activity on contact turnover have not been directly assessed. To examine the effects of acutely modulating network activity, we obtained 1 h of baseline measurements for each pair and then washed in the GABA_A antagonist bicuculline (which increases the level of firing by 2–3 fold), or of the sodium channel blocker TTX (which blocks all spiking activity; Turrigiano et al., 1998), and continued to monitor the pair for 1–2 h. Increasing activity with bicuculline ($n = 6$) had little effect on overall dynamics, and the ratio of contact gain to loss was not different from control (bicuculline, 1.04 ± 0.19 ; control, 1.13 ± 0.11). Similarly, blocking all spiking with TTX ($n = 4$) had no significant effect on the ratio of gain to loss (1.09 ± 0.21). Thus the ratio of contact gain to loss is not sensitive to acute (1–2 h) changes in the overall level of network activity. This is consistent with the observation that even prolonged treatment with TTX (48 h) does not affect the number of excitatory synapses onto these neurons at this stage *in vitro* (Wierenga et al., 2005).

We next wished to examine the dynamics of contact formation and loss for a manipulation known to alter connectivity between synaptic partners. We showed previously (using static measures) that post-synaptic CaMKII has a dual effect on presynaptic

connectivity (Pratt et al., 2003). Expressing a constitutively active form of CaMKII (T286D) in the postsynaptic neuron reduces the total number of presynaptic partners connected to T286D-expressing neurons (and decreases total synapse number), but increases the number of synaptic contacts between pairs that remain connected in an activity- and NMDA receptor-dependent manner. This suggests that activated CaMKII selects for and enhances connectivity from presynaptic partners that are effective at activating postsynaptic NMDA receptors. These synaptic changes occur without any significant alteration in total dendritic branch length or branch number (Pratt et al., 2003). CaMKII has been reported to stabilize dendritic structures in *Xenopus* tectal neurons (Wu and Cline, 1998), suggesting that this increased connectivity might be achieved through a reduction in dendritic dynamics, leading to reduced filopodial withdrawal (and thus enhanced contact stability). Alternatively, increased connectivity could be due to an increase in the rate at which new contacts are formed, or to both processes simultaneously. To differentiate between these possibilities, we measured the rates of contact loss and gain as described earlier, 16 h after transfection in pairs where only the postsynaptic neurons expressed T286D (“T286D pairs”).

In contrast to control pairs, plotting rate of gain against rate of loss for each T286D pair showed that the majority of pairs had values above the unity line (15 above, 5 below, 1 at unity), indicating that on average contact formation outstripped loss [Fig. 4(A); $n = 21$ pairs]. This resulted in a net gain of contacts over the imaging period for T286D pairs [Fig. 4(B), left; T286D significantly different from control, $p = 0.01$], consistent with our previous static data (Pratt et al., 2003). Interestingly, the percent of initial contacts that persisted throughout the experiment was not different from control [Fig. 4(B), middle; $p = 0.76$], indicating that the ratio of stable to labile contacts was not influenced by T286D. In addition, the average lifetime of the labile population was comparable between control and T286D [Fig. 4(B), right; not different from control, $p = 0.25$].

The increased ratio of gain to loss in pairs in which the postsynaptic neuron expressed T286D could be due to increased rate of gain, decreased rate of loss, or both. T286D significantly increased the rate of gain of new contacts [Fig. 4(C); $p = 0.01$], and also slightly, but not significantly, increased the rate of loss [Fig. 4(D); $p = 0.30$]. This slight increase in rate of loss was due to a higher starting number of contacts: when the rate of loss was normalized to the total number of contacts, the probability of loss was not different between control and T286D [Fig. 4(D),

inset; $p = 0.87$]. Comparing rates of gain and loss for each pair within a condition revealed that for control pairs these rates were not significantly different, whereas for T286D the rate of gain was significantly higher than the rate of loss (Fig. 5; paired t test, $p = 0.01$). Taken together, these data demonstrate that T286D increases connectivity through an increase in the rate at which new contacts form, but that once a contact forms it has a similar probability of being retained as a control contact.

Synaptically localized CaMKII is normally activated when synaptic activity opens NMDA receptors and generates calcium influx, allowing calcium/calmodulin to bind and in turn generating autophosphorylation at T286 (Lisman et al., 2002). This autophosphorylation renders the enzyme constitutively active even in the absence of calcium. The point mutation T286D mimics the autophosphorylated state of the enzyme, but like wild-type CaMKII, T286D can still be switched to a higher activity state when bound to calcium/calmodulin. We found previously that the ability of T286D to increase connectivity between pairs required its constitutive activity, but also required synaptic activation and calcium influx through NMDA receptors (Pratt et al., 2003). This suggested that T286D only enhances structural connectivity if the enzyme is both in a constitutively active state, and remains bound to calcium/calmodulin.

If so, the ability of T286D to enhance contact formation should be prevented by the selective CaMKII inhibitor KN93, which prevents calcium/calmodulin binding but does not block the constitutive activity of CaMKII. To test this we bath-applied KN93 and measured the rates of contact formation and loss in both control and T286D pairs. KN93 blocked the ability of T286D to increase new contact formation, and in the presence of KN93 the rates of gain and loss were indistinguishable between T286D and control pairs (Fig. 5; T286D + KN93, $n = 9$ pairs). In the presence of KN93 alone the rates of gain and loss were not different (Fig. 5; KN93 alone, $n = 7$ pairs, $p = 0.11$), and while there was a tendency for these rates to be lower than control, this effect was not statistically significant ($p = 0.085$). We showed previously that inhibiting endogenous CaMKII through postsynaptic expression of a peptide inhibitor (ala peptide) influences synapse number (Pratt et al., 2003), although this effect was more modest than that of T286D. This may make it difficult to detect any changes KN93 is inducing in dynamics; alternatively, KN93 does not block calcium-independent CaMKII activity and so this manipulation may not be equivalent in effect to transfection with ala peptide. Taken together, these experiments show that T286D only

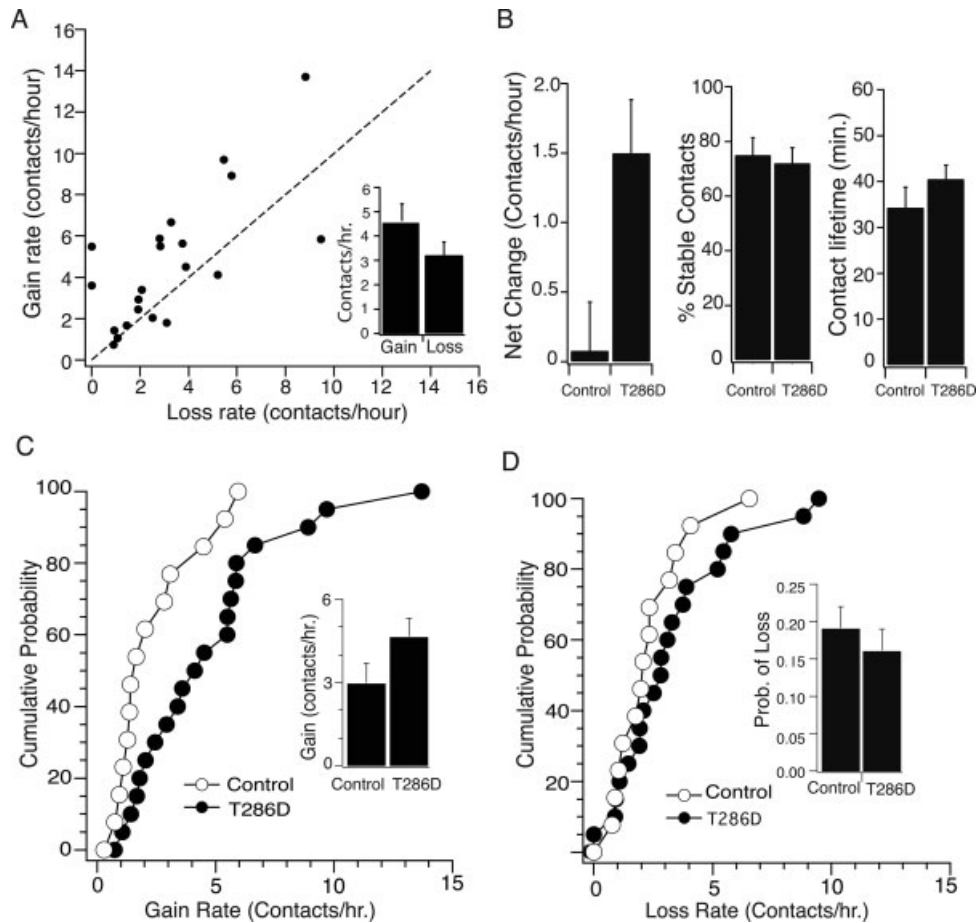


Figure 4 Postsynaptic expression of activated CaMKII (T286D) selectively increases the rate of contact gain. (A) The rates of contact gain and loss for pairs in which the postsynaptic neuron expressed T286D (“T286D pairs”), plotted for each pair. The majority of points are above the unity line (dashed line), indicating greater rates of gain than loss. Inset: rates of gain and loss averaged across T286D pairs ($n = 21$ pairs). (B) Left: net change in contact number for control and T286D pairs, over the course of 2 h; T286D significantly increased net contact gain. T286D had no effect on the proportion of stable contacts (middle), or on the average lifetime of labile contacts (right). (C) Cumulative distribution of the rate of gain of contacts for each control or T286D pair analyzed. The rate of gain was significantly higher for T286D pairs. Inset shows the average rate for the two conditions. (D) Cumulative distribution of the rate of loss of contacts for each control or T286D pair analyzed. The rate of loss was not significantly different for control and T286D pairs. Inset shows the rate of loss normalized to the total number of contacts (probability of loss). Control and T286D pairs were not significantly different.

increases contact formation if CaM binding is allowed.

An interesting observation that emerged from these experiments is that synaptic partners maintain a relatively constant fraction of connections that turn-over rapidly, with an average lifetime of around 35 min. Because we often did not follow synaptic partners for more than 2 h, we do not know how stable the more “persistent” population of synapses are, or whether these contacts also turn over on a longer time scale. Spine/filopodial turnover has been suggested to

serve a sampling function that allows neurons in developing circuits to sample many synaptic partners in a random fashion, and then selectively stabilize those contacts that are useful (Jontes and Smith, 2000). By analyzing contacts between pairs of neurons, we were able to show that the probability of any given contact being lost remained constant even under conditions (such as postsynaptic T286D expression) that enhance unitary connectivity. This suggests that turnover is subject to a stochastic process that stabilizes a set proportion of the contacts between

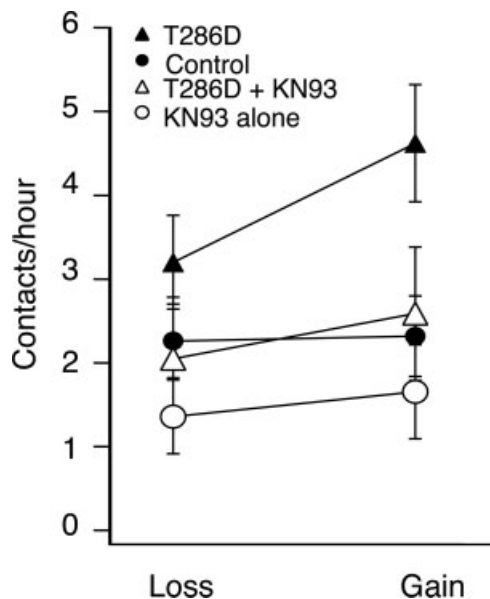


Figure 5 Increased rate of contact gain induced by T286D requires calcium–calmodulin binding. For each condition the rates of contact loss and contact gain were averaged across pairs. The rate of contact gain was significantly higher than loss for T286 (paired *t* test); for the other conditions, gain and loss were not significantly different (paired *t* tests).

partners. While the rate of contact formation is usually well matched to the rate of loss, postsynaptic T286D expression was able to uncouple these two rates and selectively increase the rate of formation. These data suggest that, at least under some conditions, formation rather than stabilization is the regulated process that leads to enhanced connectivity between synaptic partners.

The cortical neurons used here are quite young, roughly equivalent to P10–12. Counts of PSD-95 puncta density shows that while synapse density increased between DIV 4 and DIV 7 (by 61%), there was no further increase between DIV 7 and DIV 14 (1.11 ± 0.16 puncta/ $10 \mu\text{m}$ at DIV 7, and 0.99 ± 0.35 at DIV 14). This is consistent with our observation that rates of contact gain and loss are well matched at DIV 7–9, so that there is no net change in contact number. While we did not examine the rates of contact turnover at different DIV, data from *in vivo* cortex have shown that the rates of spine turnover slow considerably as animals age (Grutzendler et al., 2002; Trachtenberg et al., 2002). This suggests that the rates of contact formation and loss are also developmentally regulated, and may be much less dynamic in older neurons. It is not clear at the moment whether the mechanism for increasing con-

tact number that we have identified here, namely an increase in the rate of new contact formation induced by activated CaMKII, will generalize to periods of development in which spine dynamics have slowed.

How increasing activated CaMKII in the postsynaptic neuron enhances contact formation is not clear. We showed previously that activated CaMKII causes complete loss of contacts from some synaptic partners, while at the same time enhancing connectivity with others (Pratt et al., 2003). The experiments in this study were performed 14–16 h after CaMKII expression. At this time nearly all pairs studied underwent an increase in contact formation, suggesting that the loss of synaptic partners is largely complete before these experiments were initiated, while the enhancement of connected pairs continues. The selective nature of this enhancement suggests that it requires some signaling interaction between the pre- and postsynaptic neuron, and here we show that this signaling involves CaM binding to CaMKII. Taken together with our previous data showing that enhancement requires activity and NMDAR activation (Pratt et al., 2003), these data suggest that the synaptic partners that are retained and enhanced in the presence of activated CaMKII are those that are able to persistently generate NMDAR-mediated calcium influx in the postsynaptic neuron, and thus keep the activated kinase bound to CaM over the course of many hours. Some forms of long-lasting plasticity (such as long-term potentiation) depend upon activation of postsynaptic CaMKII (Lisman et al., 2002). Our data suggest that CaMKII-dependent changes in synaptic strength can be converted into longer lasting structural changes at synapses if there is persistent coactivity between the pre and postsynaptic neurons.

We thank Michael Walsh for technical assistance.

REFERENCES

- Bonhoeffer T, Yuste R. 2002. Spine motility: Phenomenology, mechanisms, and function. *Neuron* 35:1019–1027.
- Cohen-Cory S. 2002. The developing synapse: Construction and modulation of synaptic structures and circuits. *Science* 298:770–776.
- Deng J, Dunaevsky A. 2005. Dynamics of dendritic spines and their afferent terminals: Spines are more motile than presynaptic boutons. *Dev Biol* 277:366–377.
- Dunaevsky A, Tashiro A, Majewska A, Mason C, Yuste R. 1999. Developmental regulation of spine motility in the mammalian central nervous system. *Proc Natl Acad Sci USA* 96:13438–13443.
- Ebihara T, Kawabata I, Usui S, Sobue K, Okabe S. 2003. Synchronized formation and remodeling of postsynaptic

- densities: Long-term visualization of hippocampal neurons expressing postsynaptic density proteins tagged with green fluorescent protein. *J Neurosci* 23:2170–2181.
- Fischer M, Kaech S, Wagner U, Brinkhaus H, Matus A. 2000. Glutamate receptors regulate actin-based plasticity in dendritic spines. *Nat Neurosci* 3:887–894.
- Grutzendler J, Kasthuri N, Gan WB. 2002. Long-term dendritic spine stability in the adult cortex. *Nature* 420:812–816.
- Hua JY, Smith SJ. 2004. Neural activity and the dynamics of central nervous system development. *Nat Neurosci* 7:327–332.
- Jontes JD, Smith SJ. 2000. Filopodia, spines, and the generation of synaptic diversity. *Neuron* 27:11–14.
- Jontes JD, Buchanan J, Smith SJ. 2000. Growth cone and dendrite dynamics in zebrafish embryos: Early events in synaptogenesis imaged in vivo. *Nat Neurosci* 3:231–237.
- Konur S, Yuste R. 2004. Imaging the motility of dendritic protrusions and axon terminals: Roles in axon sampling and synaptic competition. *Mol Cell Neurosci* 27:427–440.
- Lisman J, Schulman H, Cline H. 2002. The molecular basis of CaMKII function in synaptic and behavioral memory. *Nat Rev Neurosci* 3:175–190.
- Majewska A, Sur M. 2003. Motility of dendritic spines in visual cortex in vivo: Changes during the critical period and effects of visual deprivation. *Proc Natl Acad Sci USA* 100:16024–16029.
- Marrs GS, Green SH, Dailey ME. 2001. Rapid formation and remodeling of postsynaptic densities in developing dendrites. *Nat Neurosci* 4:1006–1013.
- Matsuzaki M, Honkura N, Ellis-Davies GC, Kasai H. 2004. Structural basis of long-term potentiation in single dendritic spines. *Nature* 429:761–766.
- Niell CM, Meyer MP, Smith SJ. 2004. In vivo imaging of synapse formation on a growing dendritic arbor. *Nat Neurosci* 7:254–260.
- Oray S, Majewska A, Sur M. 2006. Effects of synaptic activity on dendritic spine motility of developing cortical layer V pyramidal neurons. *Cereb Cortex* 16:730–741.
- Pratt KG, Watt AJ, Griffith LC, Nelson SB, Turrigiano GG. 2003. Activity-dependent remodeling of presynaptic inputs by postsynaptic expression of activated CaMKII. *Neuron* 39:269–281.
- Trachtenberg JT, Chen BE, Knott GW, Feng G, Sanes JR, Welker E, Svoboda K. 2002. Long-term in vivo imaging of experience-dependent synaptic plasticity in adult cortex. *Nature* 420:788–794.
- Turrigiano GG, Leslie KR, Desai NS, Rutherford LC, Nelson SB. 1998. Activity-dependent scaling of quantal amplitude in neocortical neurons. *Nature* 391:892–896.
- Umeda T, Ebihara T, Okabe S. 2005. Simultaneous observation of stably associated presynaptic varicosities and postsynaptic spines: Morphological alterations of CA3-CA1 synapses in hippocampal slice cultures. *Mol Cell Neurosci* 28:264–274.
- Waites CL, Craig AM, Garner CC. 2005. Mechanisms of vertebrate synaptogenesis. *Annu Rev Neurosci* 28:251–274.
- Watt AJ, van Rossum MC, MacLeod KM, Nelson SB, Turrigiano GG. 2000. Activity coregulates quantal AMPA and NMDA currents at neocortical synapses. *Neuron* 26:659–670.
- Wierenga CJ, Iyata K, Turrigiano GG. 2005. Postsynaptic expression of homeostatic plasticity at neocortical synapses. *J Neurosci* 25:2895–2905.
- Wierenga C, Walsh M, Turrigiano GG. 2006. Temporal regulation of the expression locus of homeostatic plasticity. *J Neurophysiol* 96:2127–2133.
- Wong WT, Wong RO. 2000. Rapid dendritic movements during synapse formation and rearrangement. *Curr Opin Neurobiol* 10:118–124.
- Wu GY, Cline HT. 1998. Stabilization of dendritic arbor structure in vivo by CaMKII. *Science* 279:222–226.
- Yuste R, Bonhoeffer T. 2004. Genesis of dendritic spines: Insights from ultrastructural and imaging studies. *Nat Rev Neurosci* 5:24–34.
- Zhou Q, Homma KJ, Poo MM. 2004. Shrinkage of dendritic spines associated with long-term depression of hippocampal synapses. *Neuron* 44:749–757.
- Zuo Y, Yang G, Kwon E, Gan WB. 2005. Long-term sensory deprivation prevents dendritic spine loss in primary somatosensory cortex. *Nature* 436:261–265.